

## *Bam*I, *Kpn*I, and *Sal*I Restriction Enzyme Maps of the DNAs of Herpes Simplex Virus Strains Justin and F: Occurrence of Heterogeneities in Defined Regions of the Viral DNA

HILLA LOCKER AND NIZA FRENKEL\*

*Department of Biology, The University of Chicago, Chicago, Illinois 60637*

Received for publication 13 June 1979

We present the locations of the cleavage sites for the *Bam*I, *Kpn*I, and *Sal*I restriction endonucleases within the DNA molecules of herpes simplex virus type 1 (HSV-1) strains Justin and F. These restriction enzymes cleave the HSV-1 DNA at many sites, producing relatively small fragments which should prove useful in future studies of HSV-1 gene structure and function. The mapping data revealed the occurrence of heterogeneity within three regions of the viral genome including (i) the region spanning map coordinates 0.74-0.76, (ii) the ends of the large (L) DNA component, and (iii) the junction between the large (L) and the small (S) components. The heterogeneity in the ends of L and the S-L junctions of HSV-1 (Justin) and HSV-1 (F) DNAs was grossly similar to that previously reported to occur in the ends of L and the S-L junctions of the HSV-1 (KOS) DNA (M. J. Wagner and W. C. Summers, *J. Virol.* 27:374-387, 1978). Thus, cleavage of these regions with restriction endonucleases yielded sets of minor fragments differing in size by constant increments. However, the various strains of HSV-1 differed with respect to the numbers, size increments, and relative molarities of the various minor fragments, suggesting that the parameters of the heterogeneity are inherited in the structural makeup of the HSV-1 genome. The strain dependence of the pattern of heterogeneity can be most easily explained in terms of variable sizes of the terminally reiterated  $\alpha$  sequence, contained in the DNA molecules of these three strains of HSV-1.

The DNA of herpes simplex virus type 1 (HSV-1) is linear, double stranded, and approximately  $96 \times 10^6$  in molecular weight (1, 9). The DNA is composed of two components designated as L and S, each of which is bounded by an inverted repetition (15, 20, 23). The L component comprises 82% of the DNA, and consists of the unique DNA sequences  $U_L$  (molecular weight,  $67.2 \times 10^6$ ), which are bounded by the inverted repeats  $ab$  and  $b'a'$  (molecular weight,  $5.8 \times 10^6$ ). The S component comprises 18% of the DNA and is composed of the unique DNA sequences (molecular weight,  $8.9 \times 10^6$ ), which are bounded by the inverted repeats  $ac$  and  $c'a'$  (molecular weight,  $4.1 \times 10^6$ ) (20). The sequence  $\alpha$ , which is common to the S and L inverted repeats, represents the terminal reiteration of the HSV genome of estimated size between  $0.18 \times 10^6$  and  $1.0 \times 10^6$  (4, 7, 15, 19, 21, 23). The L and S components can be inverted relative to each other, and DNA extracted from virions contains equimolar amounts of four isomeric molecules, each with a unique S-L orientation (3, 5, 15, 23). These four molecules have been designated as prototype (P), inversion of S ( $I_S$ ),

inversion of L ( $I_L$ ), and inversion of both S and L ( $I_{SL}$ ).

Restriction enzyme cleavage maps of HSV-1 DNA have been constructed for a number of enzymes, including *Hind*III, *Eco*RI, *Hpa*I, *Bgl*II, and *Xba*I (2, 16, 22; G. S. Hayward, T. G. Buchman, and B. Roizman, unpublished data). The presence of the four isomeric forms of HSV DNA accounts for the unique fragment patterns produced when HSV DNA is digested with those restriction enzymes that do not have cleavage sites within the inverted repeats  $ac$  and  $ab$ . Specifically, digestion with such enzymes yields four 0.5 M fragments, arising from the four possible ends of L and S, and four 0.25 M fragments, derived from the four possible S-L junctions, as well as a number of the expected unimolar fragments derived from internal cleavage sites within the  $U_L$  and  $U_S$  sequences (5, 16, 22, 23).

Restriction enzyme analyses have also revealed that HSV-1 DNA molecules exhibit a small degree of heterogeneity (microheterogeneity) within the regions corresponding to the ends of the L component and the S-L junctions (18, 21; Hayward and Roizman, unpublished

data). Specifically, analyses of these regions with restriction enzymes which cleave the inverted repeat regions in multiple locations have revealed that the fragments originating from the L ends and from the S-L junctions can be resolved into a series of bands, differing in their size by constant size increments. This microheterogeneity was shown to result from the presence of variable numbers of copies of a 280-base pair sequence, consisting predominantly of the entire terminally reiterated sequence *a* and also including a small proportion of *b* region DNA sequences (18, 21).

In this paper we report the alignment of DNA fragments produced by cleavage of HSV-1 (Justin) and HSV-1 (F) DNAs with the *Bam*I, *Kpn*I, and *Sal*I restriction endonucleases. In contrast to most of the restriction enzymes that have previously been used to map the HSV DNA, these enzymes cleave the HSV-1 genome at a large number of sites, producing relatively small fragments. Therefore, these restriction enzyme maps should prove useful in future studies of the structure and function of the HSV-1 genome. Furthermore, our mapping studies have produced additional information concerning the occurrence of sequence microheterogeneity within defined regions of the HSV-1 genome. Details of the *Kpn*I cleavage map of HSV-1 strain 17 DNA were independently derived by A. J. Davison (quoted in reference 14).

#### MATERIALS AND METHODS

**Cells and viruses.** Human epidermoid 2 (HEp-2) cells were obtained from B. Roizman, University of Chicago. Vero cells were obtained from the American Type Culture Collection. HSV-1 (Justin) was obtained from A. Sabin. HSV-1 (F) was obtained from B. Roizman. Plaque-purified stocks of HSV-1 (Justin) and HSV-1 (F) were prepared by three sequential plaque purifications and two subsequent passages at a low multiplicity of infection ( $10^{-4}$  PFU/cell) in HEp-2 cells.

**Preparation of viral DNA.** Cultures containing  $5 \times 10^8$  Vero cells were infected for 24 h with 5 PFU/cell. The infected cells were labeled from 2 to 24 h with either 1  $\mu$ Ci of [ $^3$ H]thymidine (Amersham) per ml of 199-V medium or 70  $\mu$ Ci of [ $^{32}$ P]phosphate (Amersham) per ml of Eagle minimum essential medium minus phosphate, supplemented with 1% heat-inactivated fetal calf serum. After the infection, the cells were scraped from the bottles, rinsed with phosphate-buffered saline, and suspended in 10 ml of 0.1 M Tris-hydrochloride (pH 7.8), 0.01 M EDTA, and 0.1 M NaCl. The cells were lysed by the addition of sodium dodecyl sulfate and proteinase K to final concentrations of 0.5% and 250  $\mu$ g/ml, respectively. The cell lysates were incubated at 37°C for 3 to 4 h and were then diluted with 0.01 M Tris-hydrochloride (pH 7.8)-0.001 M EDTA (TE) to a final volume of 150 ml. After the addition of 195 g of solid CsCl and adjust-

ment of the refractive index to 1.4010, the DNA was centrifuged at 40,000 rpm for 20 h at 20°C in a Beckman Vti50 rotor. Fractions containing viral DNA were pooled and centrifuged again to equilibrium in CsCl, using the same rotor. After dialysis against TE buffer, the purified viral DNA was concentrated by ethanol precipitation.

**Restriction endonuclease analyses.** Procedures for the digestion of viral DNA with restriction endonucleases, gel electrophoresis, autoradiography, and elution of individual DNA fragments from agarose gels were as previously described (12). The molecular weights of the HSV-1 DNA fragments were determined on the basis of their mobility relative to the mobility of the *Hind*III and *Eco*RI restriction enzyme fragments of bacteriophage lambda DNA (6).

**$\lambda$  exonuclease digestion.**  $\lambda$  exonuclease was a generous gift from L. Rothman-Denes, University of Chicago. The digestion conditions were as described by Little (11).

**Hybridization to nitrocellulose strips.** Viral DNA fragments were transferred from agarose gels to BA85 nitrocellulose strips (Schleicher and Schuell) by the transfer technique of Southern (17). Hybridization of  $^{32}$ P-labeled DNA probes to these blots was performed as previously described (12).

#### RESULTS

**Derivation of the physical maps.** Figure 1 shows the electrophoretic patterns of DNA fragments produced by cleavage of  $^{32}$ P-labeled HSV-1 (Justin) and HSV-1 (F) DNAs with the *Bam*I, *Kpn*I, and *Sal*I restriction endonucleases. The ordering of these fragments within the HSV-1 (Justin) and HSV-1 (F) DNAs involved the mapping of the sites for these enzymes within the *Bgl*II restriction enzyme fragments, for which maps have been previously derived (see Fig. 2, based on Hayward et al., unpublished data). Our analyses involved the following: (i) sequential digestion of purified *Bgl*II fragments with the *Bam*I, *Kpn*I, and *Sal*I enzymes (representative gel patterns of such sequential digestions are shown in Fig. 3); (ii) hybridization of  $^{32}$ P-labeled purified *Bgl*II fragments to nitrocellulose strips containing electrophoretically separated unlabeled *Bam*I, *Kpn*I, or *Sal*I fragments (examples of such hybridizations are shown in Fig. 4); (iii) partial digestion of individual *Bgl*II fragments with limited amounts of the *Bam*I, *Kpn*I, or *Sal*I enzymes (data not shown); (iv) simultaneous digestion of the individual *Bgl*II fragments with a combination of one of the tested enzymes and a second enzyme (either *Eco*RI, *Hind*III, or *Hpa*I) for which the cleavage sites within HSV-1 DNA have been previously mapped (data not shown). On the basis of these analyses we have derived the *Bam*I, *Kpn*I, and *Sal*I cleavage maps shown in Fig. 5 and 6 for HSV-1 (Justin) and HSV-1 (F) DNAs, respectively.

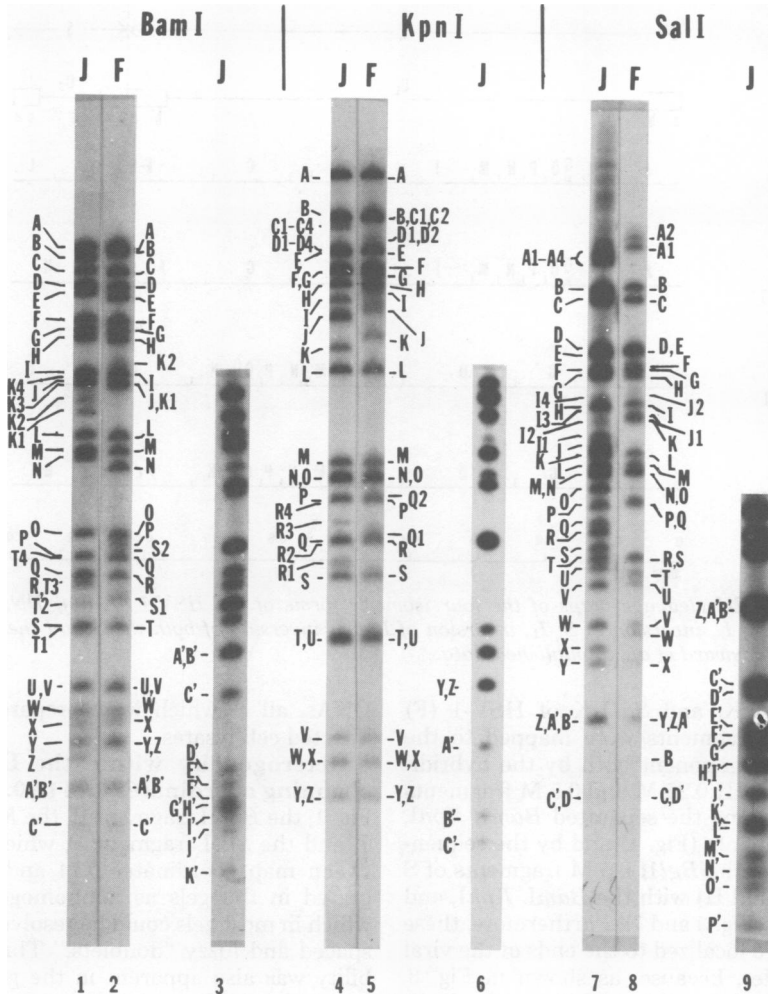


FIG. 1. Digestion of HSV-1 (Justin) and HSV-1 (F) DNAs with the *Bam*I, *Kpn*I, and *Sal*I restriction endonucleases. Autoradiograms of electrophoretically separated <sup>32</sup>P-labeled fragments of HSV-1 (Justin) (J) and HSV-1 (F) (F) DNAs digested with *Bam*I, *Kpn*I, and *Sal*I enzymes. Tracks 3, 6, and 9 represent stronger autoradiographic exposures of similar gels, to show the groups of smaller fragments.

**Minor fragments derived from HSV-1 (Justin) and HSV-1 (F) DNAs.** Because the *Bam*I and *Sal*I enzymes cleave within the inverted repeat regions of both the L (*ab-a'b'*) and the S (*ac-a'c'*) components of HSV-1 DNA, we expected that all of the fragments produced by cleavage of HSV-1 DNA with these enzymes would appear in unit molarities. Furthermore, in the case of the *Kpn*I enzyme, which cleaves within the inverted repeat of the L component (*ab*) but does not cleave within the inverted repeat of the S component (*ac*), we expected that the two fragments generated from the ends of S would appear in 0.5 M quantities, whereas all remaining fragments would appear in unit

molarities. However, as seen in Fig. 1, the gel patterns of HSV-1 (Justin) and HSV-1 (F) DNAs cleaved with the *Bam*I, *Kpn*I, and *Sal*I enzymes each contained four sets of fragments that were present in less than unit molarities. These four sets of minor fragments will be discussed separately below and include those fragments derived from (i) the ends of S, (ii) the U<sub>1</sub> sequences spanning map coordinates 0.74 to 0.76, (iii) the ends of L, and (iv) the S-L junctions.

**Fragments generated from the ends of S.** The first set of fragments that appeared to be present in lower than unit molarity included the fragments *Bam*I-R, *Kpn*I-I and K, and *Sal*I-J of HSV-1 (Justin) DNA and the fragments *Bam*I-

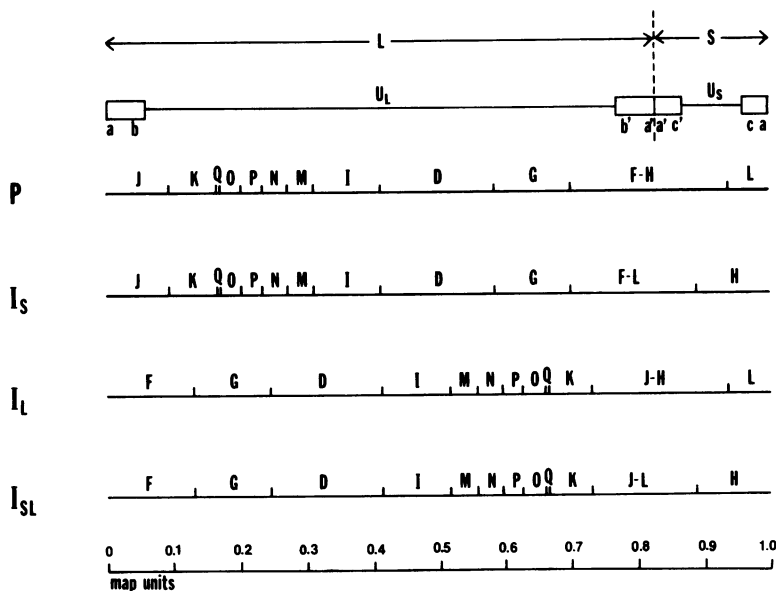


FIG. 2. The *Bgl*II cleavage maps of the four isomeric forms of the HSV-1 (Justin) DNA. P, prototype arrangement (13); I<sub>S</sub>, inversion of S; I<sub>L</sub>, inversion of L; I<sub>SL</sub>, inversion of both the S and the L components. Data are from Hayward et al., unpublished data.

P, *Kpn*I-I and K, and *Sal*I-K of HSV-1 (F) DNAs. These fragments were mapped to the ends of the S component both by the hybridization of the *Bgl*II 0.25 M and 0.5 M fragments to blots containing the separated *Bam*I, *Kpn*I, and *Sal*I fragments (Fig. 4) and by the sequential digestion of the *Bgl*II 0.5 M fragments of S (fragments L and H) with the *Bam*I, *Kpn*I, and *Sal*I enzymes (Fig. 3 and 7). Furthermore, these fragments were localized to the ends of the viral DNA molecules, because, as shown in Fig. 8, they preferentially disappeared from the gel patterns when the cleavage with the restriction enzymes was preceded by limited digestion of the DNAs with bacteriophage lambda exonuclease. Because the fragments generated from the ends of S were unique and homogeneous in size, their reduced molarities could not have resulted from the occurrence of size variability within the ends of the S regions of HSV-1 (Justin) and HSV-1 (F) DNA. Instead, the reduced molarities for the S end fragments are consistent with the previous observation of Jacob et al. (8), who have reported that HSV-1 DNA prepared from infected cell nuclei displayed increased molarities of the S-L junction fragments and reduced molarities of the S and L end fragments, due to the presence of concatemeric, head-to-tail replicative forms of viral DNA. In line with this explanation is our experience that the molarities of the S end fragments varied in different preparations of HSV-1 (Justin) and HSV-1 (F)

DNAs, all of which were prepared from total infected cell lysates.

**Heterogeneity within the U<sub>1</sub> sequences spanning coordinates 0.74 to 0.76.** As seen in Fig. 1, the *Bam*I fragment B, the *Kpn*I fragment J, and the *Sal*I fragment F, which overlap between map coordinates 0.74 and 0.76, all migrated in the gels as nonhomogeneous bands which in most gels could be resolved into closely spaced and fuzzy "doublets." This same variability was also apparent in the gel patterns of fragments produced by the sequential cleavage of the *Bgl*II fragment F, which maps in this region, with the *Bam*I, *Kpn*I, and *Sal*I enzymes (Fig. 3 and 7). In the case of HSV-1 (F) DNA, approximately 65% of the radioactivity was found in the faster-migrating band of each doublet, whereas in the case of HSV-1 (Justin) DNA the faster-migrating band contained no more than 10% of the radioactivity. In addition, it should be noted that virus stocks made from two plaque-purified isolates, propagated from a common stock of HSV-1 (Justin), were found to differ slightly with respect to the sizes of the corresponding *Bam*I, *Kpn*I, and *Sal*I fragments of this region (data not shown). All of these observations indicate the occurrence of variability within the sequences spanning map coordinates 0.74 to 0.76 of HSV-1 DNA.

**Heterogeneity within the ends of L and the S-L junctions.** As seen in Fig. 1 and summarized in Table 1, the cleavage of HSV-1 (Jus-

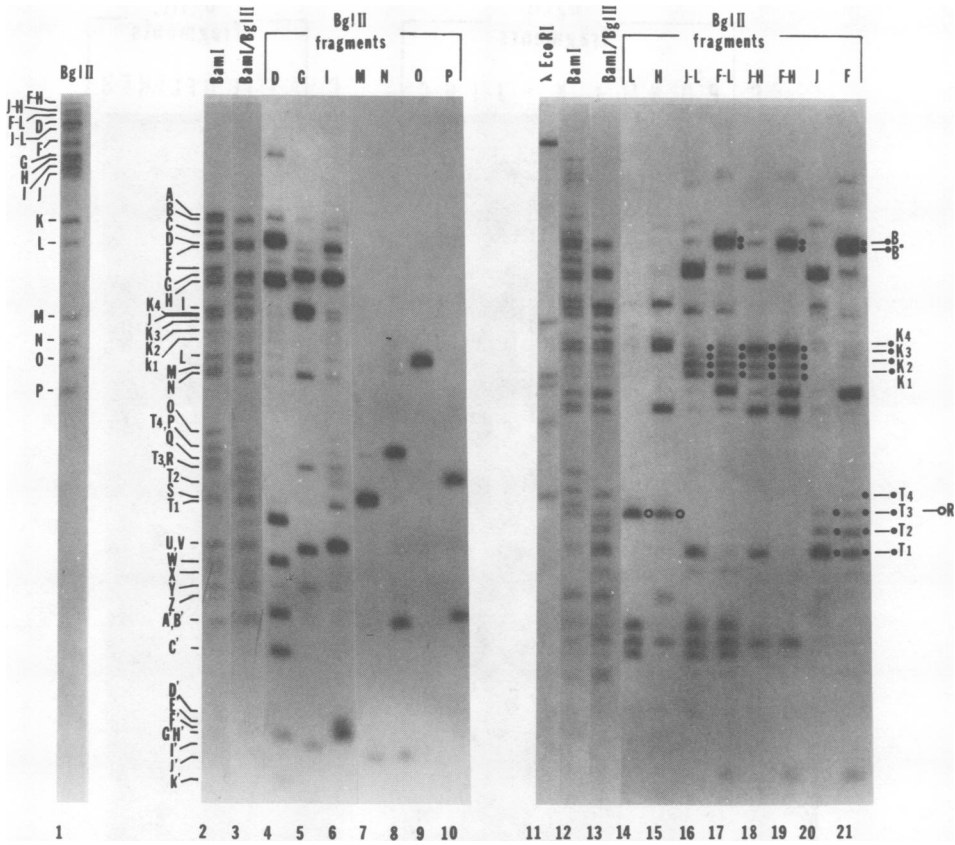


FIG. 3. Sequential cleavage of the individual *Bgl*II fragments of HSV-1 (Justin) DNA with the *Bam*I enzyme. Autoradiograms of agarose gels containing the electrophoretically separated DNA fragments produced by cleavage of the various *Bgl*II fragments (shown in track 1) with the *Bam*I enzyme (tracks 4-10 and 14-21). The fragments produced in each of these digests were identified by comparing their mobility to the mobility of fragments generated by the cleavage of HSV-1 (Justin) DNA with the *Bam*I enzyme alone (tracks 2 and 12) and in combination with the *Bgl*II enzyme (tracks 3 and 13). Also shown is the *Eco*RI digest of bacteriophage  $\lambda$  DNA, which was included in the right gel (track 11).

tin) and HSV-1 (F) DNAs with the *Bam*I, *Kpn*I, and *Sal*I enzymes generated, in each case, two additional groups of minor fragments. The fragments within each group migrated in the gels as closely spaced but distinct bands. The assignment of map coordinates to these two groups of minor fragments was based on the following data. (i) As seen in Fig. 4, the *Bgl*II 0.5 M and 0.25 M fragments were found to hybridize to both sets of minor fragments. (ii) In each case, the group of smaller minor fragments was generated by cleavage of the *Bgl*II 0.5 M fragments of the L component (*Bgl*II fragments F and J), whereas the group of the larger minor fragments was generated upon cleavage of each of the *Bgl*II 0.25 M fragments (*Bgl*II fragments FH, JH, FL, and JL) (Fig. 3 and 7). (iii) The digestion of HSV-1 (Justin) and HSV-1 (F) DNAs with  $\lambda$

exonuclease, prior to their cleavage with the restriction enzymes, resulted in the disappearance of the group of the smaller minor fragments, indicating that they are located at the ends of the DNA molecules (Fig. 8). On the basis of the above, we concluded that the group of small minor fragments produced by each enzyme was derived from the ends of the L component, whereas each group of the larger minor fragments arose from the S-L junctions.

In addition to allowing the localization of the minor fragments generated from the ends of L and the S-L junctions, the sequential digestion of the *Bgl*II 0.5 M and 0.25 M fragments with the *Bam*I, *Kpn*I, and *Sal*I enzymes provided information concerning the sizes, abundances, and strain differences of these various minor fragments. These data are summarized in Tables

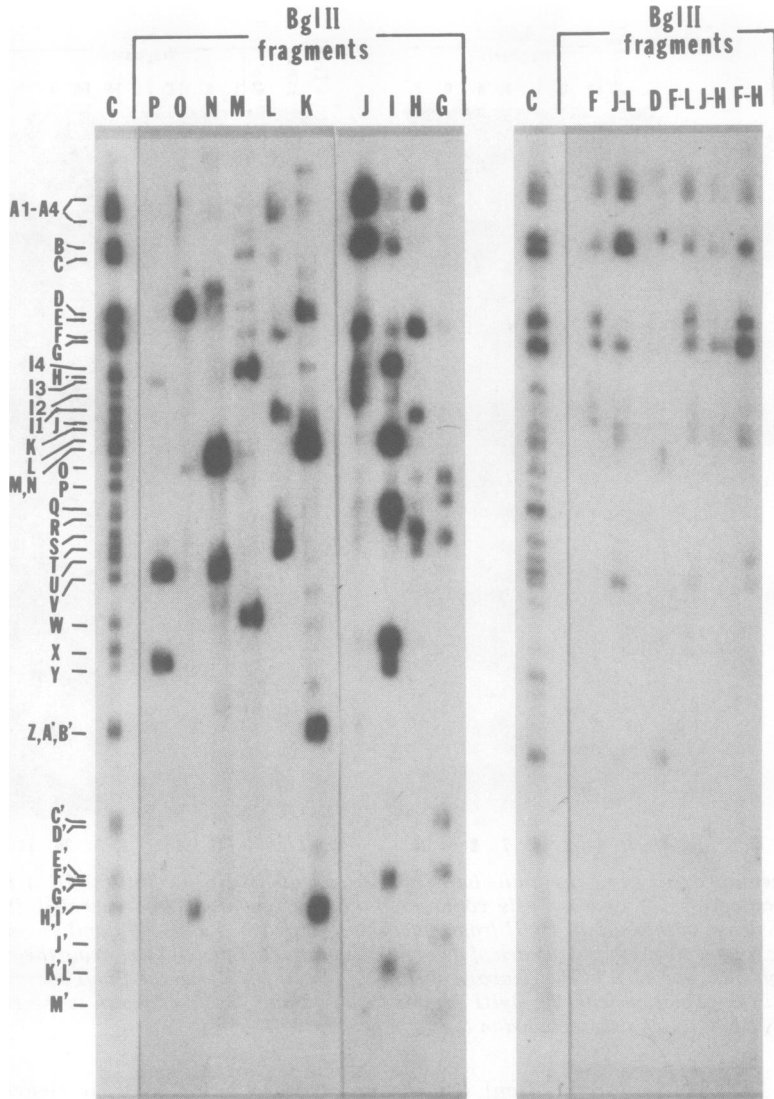


FIG. 4. Hybridizations of individual *Bgl*II fragments of HSV-1 (Justin) DNA to nitrocellulose blots containing the electrophoretically separated *Sal*I fragments of HSV-1 (Justin) DNA. The  $^{32}$ P-labeled *Bgl*II fragments of HSV-1 (Justin) DNA were hybridized, as described in the text, to the nitrocellulose strips containing the separated *Sal*I fragments of HSV-1 (Justin) DNA. The hybridized bands were identified by comparison with control replicate nitrocellulose blots which were hybridized to  $^{32}$ P-labeled whole HSV-1 (Justin) DNA (C).

1 and 2 and reveal the following. (i) The heterogeneity in the ends of the L region and the S-L junctions of HSV-1 DNA seemed to be strain specific in that HSV-1 (Justin) and HSV-1 (F) DNAs differed with respect to both the number and the size increments of the minor fragments generated from these regions. Specifically, in the case of HSV-1 (F) DNA, two or sometimes three types of L end fragments could be identified in each of the two possible orientations of the L

component (i.e., in sequential digests of the *Bgl*II fragments F and J with the *Bam*I, *Kpn*I, and *Sal*I enzymes; see Fig. 7). These L end fragments differed in their sizes by 515 base pairs. Similarly, three different types of S-L junction fragments could be identified from each of the four possible S-L junctions of HSV-1 (F) DNA (i.e., following cleavage of each of the four *Bgl*II 0.25 M fragments; see Fig. 7). These three S-L junction fragments differed in their sizes by

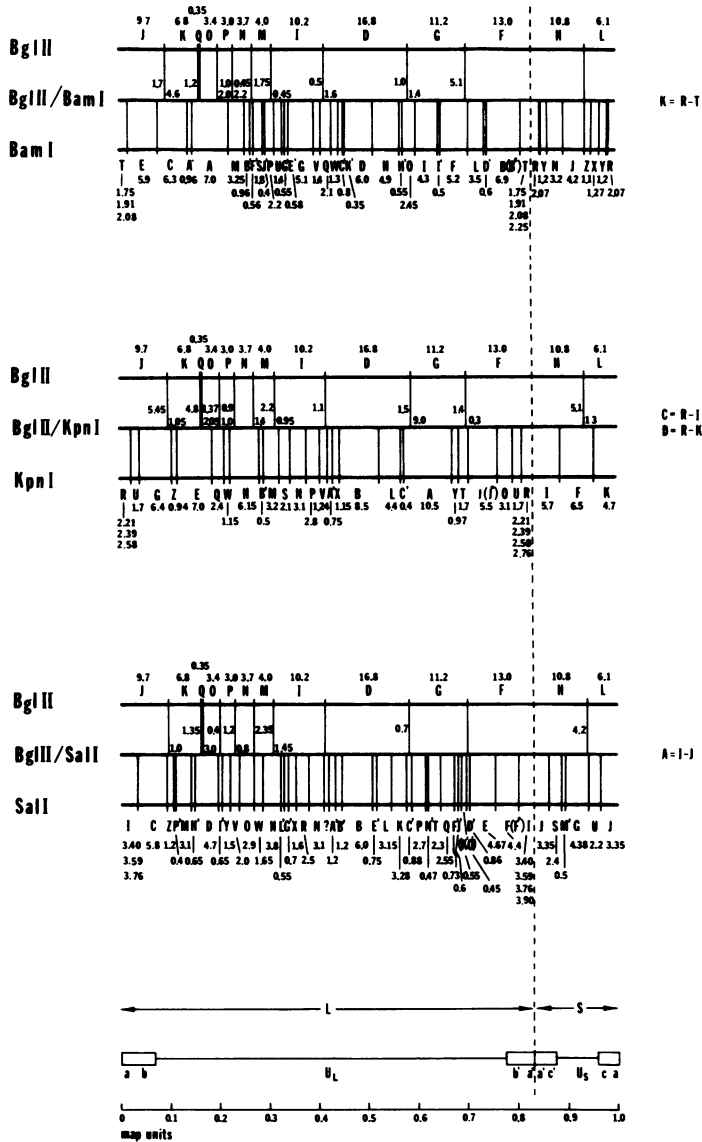


FIG. 5. The *BamI*, *KpnI*, and *Sall* restriction enzyme cleavage maps of HSV-1 (Justin) DNA. The numbers represent molecular weights  $\times 10^6$ .

485-base pair increments. In the case of the HSV-1 (Justin) DNA, four minor fragments were generated by cleavage of the *BglII* fragment F (located at the L end of the  $I_L/I_{SL}$  orientations). In contrast, only the smaller three of these four L end minor fragments could be detected after cleavage of the *BglII* fragment J (the L ends of the  $P/I_S$  orientations), even after prolonged autoradiographic exposures (Fig. 3 and 7). The average size increment between the four types of L end fragments was found to be 256 base pairs. An identical set of four minor

fragments was generated from each of the four *BglII* 0.25 M fragments (Fig. 3 and 7), and these differed by size increments of 253 base pairs. (ii) As seen in Table 1, there was an apparent discrepancy between the observed sizes of the S-L junction fragments and their expected sizes, if they were to arise from a simple fusion of the S region end fragments with the corresponding L region end fragments. Specifically, in HSV-1 (Justin) DNA the junction fragments were shorter than expected by approximately 125 base pairs, whereas in HSV-1 (F) DNA they

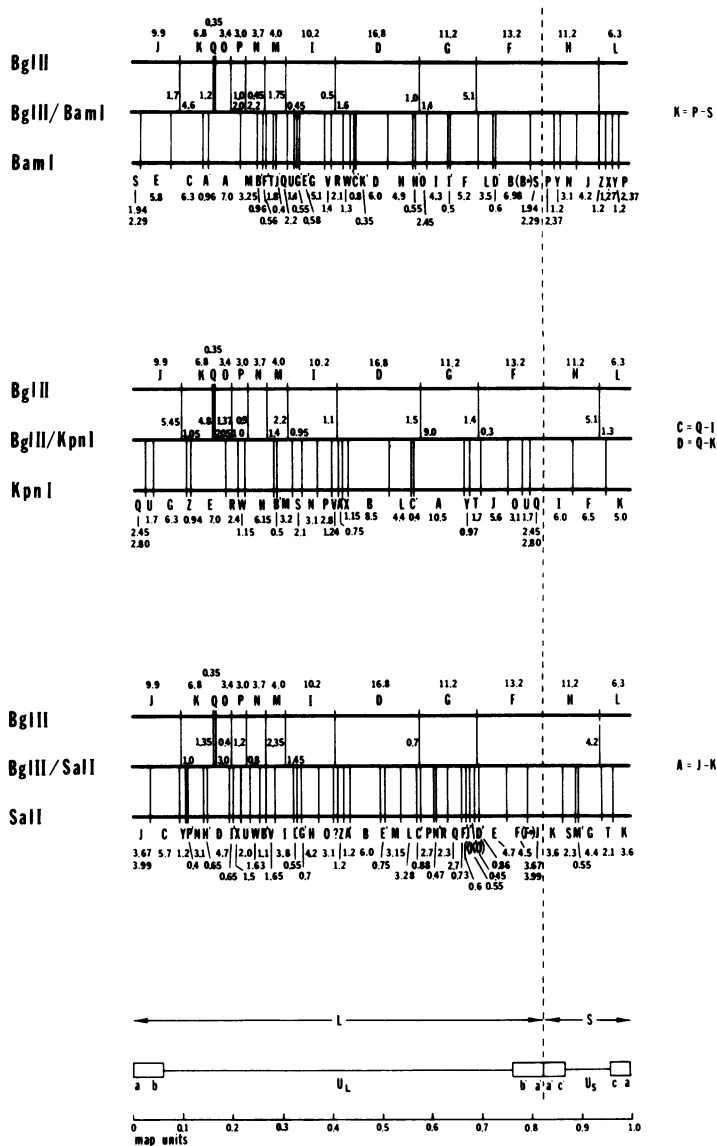


FIG. 6. The *BamI*, *KpnI*, and *SalI* restriction enzyme cleavage maps of HSV-1 (F) DNA. The numbers represent molecular weights  $\times 10^6$ .

were short by approximately 280 base pairs. This observation suggests that certain end-region sequences seem to be deleted at the S-L junctions, and that the extent of these deletions is strain specific. (iii) In all four configurations of HSV-1 (Justin) and HSV-1 (F) DNAs, the largest proportion of the molecules terminated with the smallest L end fragment, whereas molecules with increasing size of L end fragments gradually decreased in abundance. (iv) As seen in Table 2, in both the HSV-1 (Justin) and HSV-1 (F) DNAs there was no direct correlation between

the molarities of the L end fragments and the corresponding S-L junction fragments.

DISCUSSION

In this paper we have described the mapping of HSV-1 (Justin) and HSV-1 (F) DNAs with the *BamI*, *KpnI*, and *SalI* restriction endonucleases. Because most of the HSV-1 DNA fragments generated by these enzymes are relatively small, they migrate in regions of agarose gels which provide high resolution and therefore allow relatively accurate determinations of molec-



ular weights. Thus, we expect that these cleavage maps will be useful in future studies of the structure and function of the HSV-1 genome.

One characteristic feature of the HSV-1 DNA that was apparent from our mapping analyses was the occurrence of minor heterogeneities in size within defined regions of the viral genome. These heterogeneous regions include (i) the sequences within  $U_1$ , spanning coordinates 0.74 to 0.76; (ii) the ends of the L component; and (iii) the S-L junctions.

The nature and significance of the microheterogeneity within the  $U_1$  sequences is at present unknown. It is noteworthy, however, that analyses of the DNA of a third HSV-1 strain (VR-3) with the *Bam*I, *Kpn*I, and *Sal*I enzymes have revealed the existence of a similar  $U_1$  sequence microheterogeneity. Thus, it appears that the variability between map coordinates 0.74 and 0.76 is a common property of a number of HSV-

1 strains, and that it most likely reflects an inherent structural or functional feature of the DNA sequences located between these map coordinates.

The microheterogeneity of the ends of the L component and the S-L junctions has been previously characterized by Summers and Skare (18) and Wagner and Summers (21), who made use of restriction enzymes that have multiple cleavage sites within the inverted repeat regions of HSV-1 (KOS) DNA. Their data revealed that the microheterogeneity at the ends of L and at the S-L junctions was due to the presence of variable numbers of copies of a 280-base pair sequence, composed of the entire terminally reiterated region *a* and a small stretch of the adjacent *b* region DNA sequences. The finding that the ends of S (containing *ac* sequences) did not display microheterogeneity similar to that observed for the ends of L (containing *ab* se-

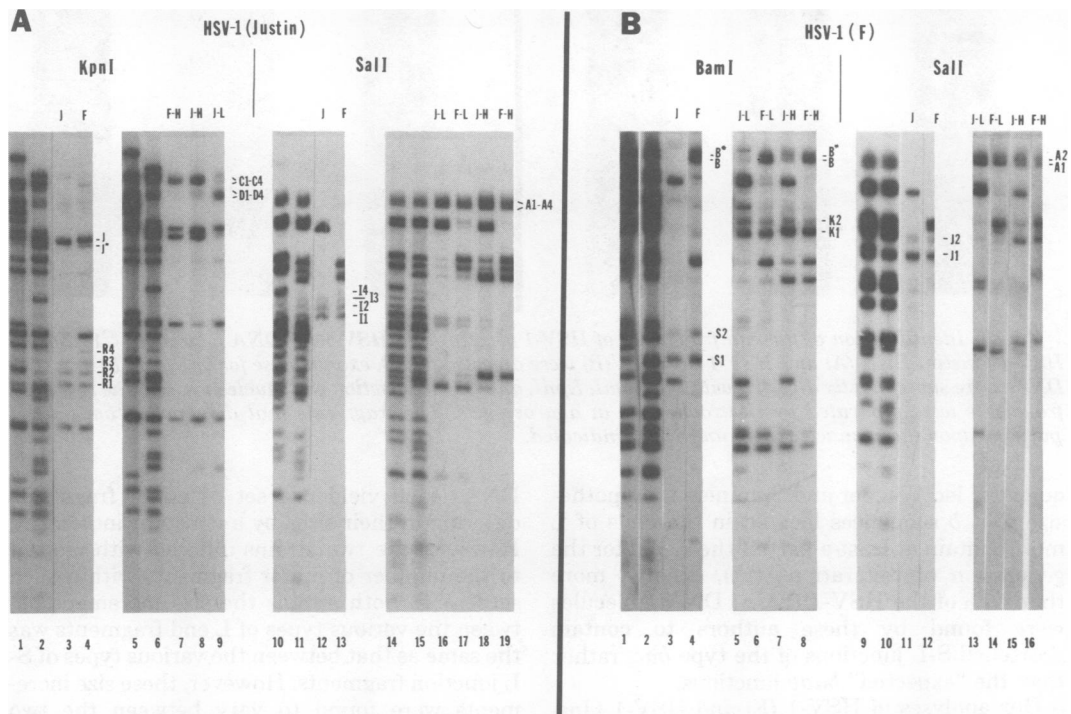


FIG. 7. The microheterogeneities within HSV-1 (Justin) and HSV-1 (F) DNAs. (A) Autoradiograms of electrophoretically separated fragments generated by digestion of the *Bgl*II 0.5 M fragments of the L component (J and F) and the *Bgl*II 0.25 M fragments (F-H, J-H, J-L, and F-L) of HSV-1 (Justin) DNA with the *Kpn*I and *Sal*I enzymes. Tracks 1, 5, 10, and 14 represent cleavage of intact HSV-1 (Justin) DNA with the *Kpn*I or *Sal*I enzymes. Tracks 2, 6, 11, and 15 represent double digestion of intact HSV-1 (Justin) DNA with the *Bgl*II and the *Kpn*I or *Sal*I enzymes. (B) Autoradiograms of electrophoretically separated fragments generated by digestion of the isolated *Bgl*II 0.5 M fragments (J and F) and the *Bgl*II 0.25 M fragments (J-L, F-L, J-H and F-H) of HSV-1 (F) DNA with the *Bam*I and *Sal*I enzymes, respectively. Tracks 2 and 10, double digestion of the intact HSV-1 (F) DNA with the *Bam*I and *Sal*I enzymes, respectively. Tracks 1 and 9, cleavage of the intact HSV-1 (F) DNA with the *Bam*I and *Sal*I enzymes, respectively. Tracks 2 and 10, double digestion of the intact HSV-1 (F) DNA with the *Bgl*II and the *Bam*I or *Sal*I enzymes. Minor fragments related to the microheterogeneities at the L ends, S-L junctions, and the  $U_1$  region spanning coordinates 0.74–0.76 are indicated.

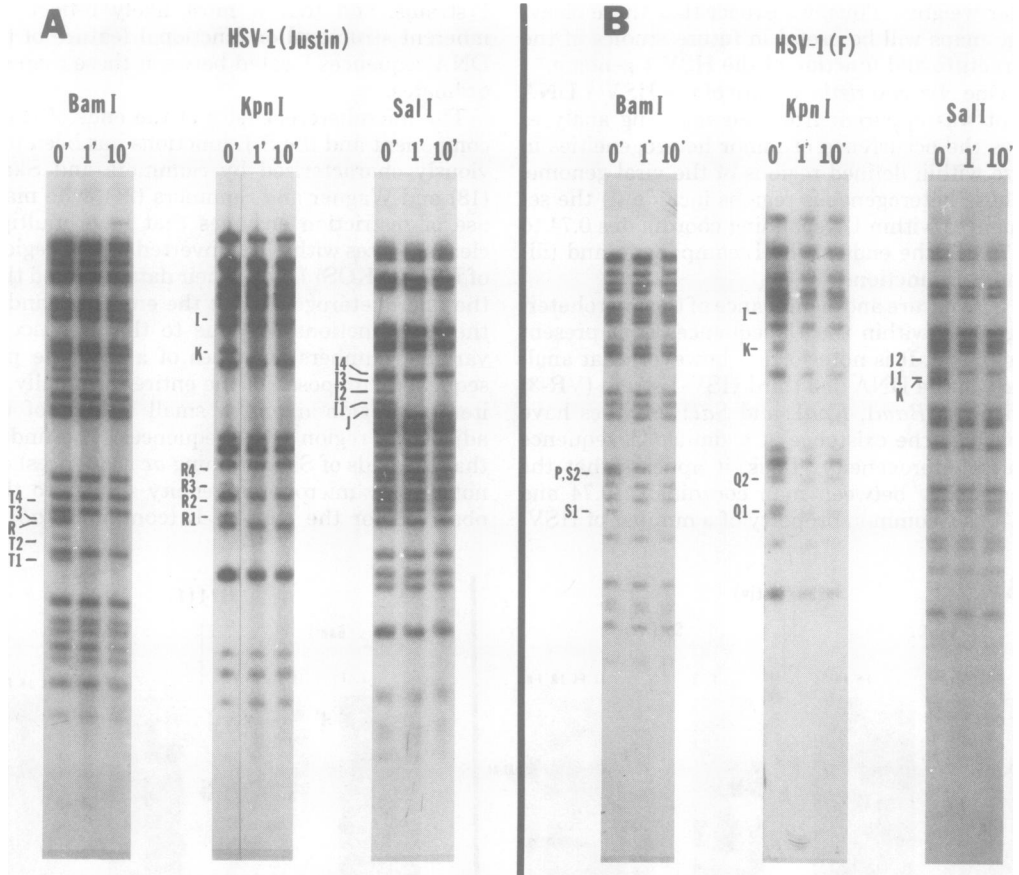


FIG. 8. Identification of the end fragments of HSV-1 (Justin) and HSV-1 (F) DNA molecules.  $^{32}\text{P}$ -labeled HSV-1 (Justin) DNA (A) and HSV-1 (F) DNA (B) were digested with  $\lambda$  exonuclease for 0, 1, and 10 min. The DNAs were subsequently digested with the *Bam*I, *Kpn*I, and *Sal*I restriction endonucleases, and the resultant fragments were separated by electrophoresis in agarose gels. The fragments that disappear from the gel patterns upon the exonuclease treatment are indicated.

quences) led Wagner and Summers to hypothesize that *b* sequences located in the ends of L must contain at least a part of the signal for the generation of reiterations (21). Finally, more than 50% of the HSV-1 (KOS) DNA molecules were found by these authors to contain shortened S-L junctions of the type *bac*, rather than the "expected" *baac* junctions.

Our analyses of HSV-1 (F) and HSV-1 (Justin) DNAs with the *Bam*I, *Kpn*I, and *Sal*I enzymes have revealed the existence of microheterogeneity grossly similar to that reported by Summers and co-workers (18, 21) for HSV-1 (KOS) DNA. However, we have also found that certain parameters of this microheterogeneity were strain dependent, as follows. (i) As was found for the HSV-1 (KOS) DNA, the restriction enzyme cleavages of the ends of L and S-L junctions of HSV-1 (Justin) and HSV-1 (F)

DNAs each yielded a set of minor fragments differing in their sizes by a constant increment. However, the two strains differed with respect to the number of minor fragments within each set. (ii) In both strains the size increment between the various types of L end fragments was the same as that between the various types of S-L junction fragments. However, these size increments were found to vary between the two strains. Specifically, our measurements of the size increment between the minor fragments of HSV-1 (Justin) DNA was 255 base pairs [in good agreement with that reported for HSV-1 (KOS) DNA], whereas the size increment between the various minor fragments of HSV-1 (F) DNA was significantly larger (approximately 500 base pairs). (iii) The S-L junction fragments were uniformly smaller than the sums of the sizes of the corresponding S and L end fragments, in

TABLE 1. Size increments between the minor fragments generated from the L ends and the S-L junctions of HSV-1 (Justin) and HSV-1 (F) DNAs

Site	<i>Bam</i> I			<i>Kpn</i> I			<i>Sa</i> I			Avg size increment <sup>b</sup> (×10 <sup>6</sup> )	Expected size <sup>c</sup> (10 <sup>6</sup> )	Discrepancy between expected and observed sizes (×10 <sup>6</sup> )
	Fragment	Size (×10 <sup>6</sup> )	Increment <sup>a</sup> (×10 <sup>6</sup> )	Fragment	Size (×10 <sup>6</sup> )	Increment <sup>a</sup> (×10 <sup>6</sup> )	Fragment	Size (×10 <sup>6</sup> )	Increment <sup>a</sup> (×10 <sup>6</sup> )			
HSV-1 (Justin) L ends	T1	1.75	0.16	R1	2.21	0.18	I1	3.40	0.19	0.18		
	T2	1.91	0.17	R2	2.39	0.19	I2	3.59	0.14			
	T3	2.08	0.17	R3	2.58	0.18	I3	3.76	0.14			
	T4	2.25		R4	2.76		I4	3.90				
HSV-1 (Justin) S-L junctions	K1	3.74	0.15		ND <sup>d</sup>			ND <sup>d</sup>		3.82	0.08	
	K2	3.89	0.18							3.98	0.09	
	K3	4.07	0.17							4.15	0.08	
	K4	4.24								4.32	0.08	
HSV-1 (F) L ends	S1	1.94	0.35	Q1	2.45	0.35	J1	3.67	0.32	0.34		
	S2	2.29		Q2	2.80		J2	3.99				
HSV-1 (F) S-L junctions	K1	4.14	0.32		ND <sup>d</sup>			ND <sup>d</sup>		4.31	0.17	
	K2	4.46								4.66	0.20	

<sup>a</sup> Differences in sizes of adjacent fragments.

<sup>b</sup> Average size increments determined for the corresponding *Bam*I, *Kpn*I, and *Sa*I fragments.

<sup>c</sup> Expected sizes of the various S-L junction fragments if their molecular weights corresponded to the sums of the molecular weights of the S end fragment and the corresponding L end fragments. The size of the S end fragment of HSV-1 (Justin) DNA (*Bam*I-R) is  $2.07 \times 10^6$ ; the size of the S end fragment of HSV-1 (F) DNA (*Bam*I-P) is  $2.37 \times 10^6$ .

<sup>d</sup> Accurate determinations of the molecular weights of the *Kpn*I and *Sa*I S-L junction fragments could not be obtained, because these relatively large fragments migrated in nonlinear regions of the agarose gels.

support of the conclusion of Wagner and Summers that sequences are deleted from the S-L junctions. However, the difference between the observed and the expected sizes of the S-L junction fragments was smaller in HSV-1 (Justin) DNA (125 base pairs) than in either HSV-1 (F) DNA (280 base pairs) or HSV-1 (KOS) DNA (280 base pairs, as reported by Wagner and Summers). (iv) In both HSV-1 (Justin) and HSV-1 (F) DNAs the minor fragments generated from the ends of L and from the four S-L junctions differed in their relative molarities.

The significance of the observation that various strains of HSV-1 seem to differ with respect to the microheterogeneity occurring at their L ends and S-L junctions is at present unknown. However, the existence of these strain differences is most easily explained by postulating that various strains of HSV-1 contain different amounts of sequences between the L end of the molecule and the unique site within the *b* region which, as discussed above, has been postulated to be involved in the generation of the reiterations (21). This difference in size could be due either to variable sizes of the terminally reiterated *a* sequences, to variable amounts of the *b* region DNA sequences contained within this area, or to both. Although we cannot distinguish between these two possibilities on the basis of

the data presented above, there are three previous observations which suggest that the strain heterogeneity is due, at least in part, to the variable amounts of *a* region DNA sequences contained in these three strains of HSV-1. First, restriction enzyme fragments generated from both the L and the S ends of HSV-1 (F) DNA have been shown to be larger than those generated from the ends of HSV-1 (Justin) DNA (Hayward et al., unpublished data; and the *Bam*I, *Kpn*I, and *Sa*I cleavage maps in this paper). Second, Wadsworth et al. (19) have reported that, whereas 46% of HSV-1 (F) DNA molecules were capable of forming circles after digestion with bacteriophage  $\lambda$  exonuclease, only 12% of HSV-1 (Justin) DNA molecules were circularized under similar conditions. This difference might be explained in terms of a larger terminal reiteration in HSV-1 (F) DNA, which facilitates the formation of circles after the exonuclease digestion. Finally, a number of conflicting reports have recently been published regarding the size of the terminal reiteration of the HSV-1 genome. Specifically, the size estimated for the terminally reiterated region of HSV-1 (KOS) DNA, which was obtained on the basis of restriction enzyme analyses (21), was significantly smaller than size estimates for the terminal reiteration region for HSV-1 (Patton)

TABLE 2. Molar ratios of the minor fragments generated from the L ends and the S-L junctions of HSV-1 (Justin) and HSV-1 (F) DNAs

Virus strain	Fragment no. <sup>a</sup>	L end fragment molar ratios <sup>b</sup>		S-L junction fragment molar ratios <sup>c</sup>			
		P/I <sub>s</sub> (BglII-J)	I <sub>1</sub> /I <sub>s1</sub> (BglII-F)	P (BglIII-FH)	I <sub>s</sub> (BglIII-FL)	I <sub>1</sub> (BglIII-JH)	I <sub>s1</sub> (BglIII-JL)
HSV-1 (Justin)	1	0.59 <sup>d</sup>	0.49	0.31	0.31	0.29	0.32
	2	0.33	0.35	0.34	0.32	0.35	0.39
	3	0.07	0.13	0.35 <sup>d</sup>	0.23	0.36 <sup>d</sup>	0.21
	4	—	0.04		0.14		0.08
HSV-1 (F)	1	0.89	0.78	0.57	0.69	0.53	0.56
	2	0.11	0.22	0.43	0.31	0.47	0.44

<sup>a</sup> 1 to 4 denote the fragments, in increasing sizes, within each set of minor fragments.

<sup>b</sup> The BglII fragments arising from the L ends of the DNA, in the orientations shown, were cleaved with the *Bam*I, *Kpn*I, or *Sal*I enzymes. The relative densities of the various resultant bands were determined from densitometric scans of the autoradiograms using a Transidyne 2955 densitometer, equipped with an automatic integrator. The molar ratio of a given minor fragment relative to the other minor fragments in the same set was calculated from the fractional density and the fractional molecular weight of that fragment, in the following way: molar ratio = (fractional density of the fragment/sum of the fractional densities of the minor fragments in the same set)/(molecular weight of the fragment/sum of the molecular weights of the minor fragments in the same set). The average values obtained for the *Bam*I, *Kpn*I, and *Sal*I fragments are shown.

<sup>c</sup> The BglII fragments arising from the S-L junctions of the DNA, in the orientations shown, were cleaved with the *Bam*I enzyme, and the molar ratios of the resultant minor fragments were calculated as described above.

<sup>d</sup> A major fragment of size  $1.7 \times 10^6$  comigrated with the minor *Bam*I-T1 fragment in the *Bam*I digest of the BglII fragment J. The molarity of *Bam*I-T1 was determined by subtracting the equivalent of 1 M from the composite molarity of the band. A similar allowance was made to account for the comigration of the major fragment *Bam*I-J with the minor fragment *Bam*I-K4 in the *Bam*I digest of the BglII fragments JH and FH. The sum of the molar ratios of the *Bam*I-K3 and K4 fragments is shown, because the presence of the unrelated *Bam*I-J fragment did not allow adequate resolution of these bands in the densitometric scanning.

DNA (4, 7) and for HSV-1 (F) DNA (19), which were obtained in separate laboratories through the use of the electron microscopy approaches. Although the use of nonanalogous techniques in these studies does not permit a strictly valid comparison, it is possible that the discrepancies between these measurements reflect true differences in the sizes of the terminal reiterations in the DNA molecules of these various HSV-1 strains.

There are currently no data concerning the nature of the events leading to the generation of microheterogeneities at the L ends and at the S-L junctions. However, the observation that sequence reiteration is present in a significant proportion of plaque-purified viral DNA molecules of different strains of HSV-1 suggests that the generation of the microheterogeneity is a highly probable event, the potential for which is inherent in the genetic makeup of various HSV-1 strains. It is also unclear whether, within each strain, the similar heterogeneities of the L ends and S-L junctions are independently generated, or instead are generated first at one of these regions and are then transposed to the second region. Pertinent to this question are recent findings based on genetic analyses (10), which

suggest the occurrence of obligatory identity of the *a* region DNA sequences present at the L ends, S ends, and S-L junctions. These studies have shown that a mutation in one *a* region, as well as wild-type DNA sequences used to rescue this mutation, are copied to other *a* regions of the DNA. However, if the L end reiterations are copied from or into the S-L junctions, this copying seems to differ at least in two respects from that responsible for the genetic identity of the various sets of *a* region DNA sequences (10). First, the microheterogeneity is not transposed from the S ends, at least in the HSV-1 strains discussed in this paper. Second, although our current data do not permit us to determine whether molecules containing a certain number of reiterations at the L ends contain the same number of reiterations at the S-L junctions, the data do show that the relative molarities of the minor fragments that are generated from the ends of the L component do not correlate well with the relative molarities of the S-L junction fragments. This finding might suggest that the end region reiterations are not simply copied en masse either from or into the S-L junctions. However, as noted above, our analyses have been performed on viral DNA extracted from

total cell lysates which, in addition to mature unit-length viral DNA molecules, most likely also contain concatemeric replicative forms of viral DNA (8). Thus, the relationship between the structural features of the ends of L and the S-L junctions must be reexamined using DNA extracted from virions. These studies are currently in progress.

#### ACKNOWLEDGMENTS

We thank Barbara Burckart and Ida Schaffer for excellent technical assistance, Jeffrey M. Leiden and David Knipe for most helpful discussions, and L. Rothman-Denes for providing the  $\lambda$  exonuclease.

This study was supported by Public Health Service Research grants AI-15488 and CA-19264 from the National Institutes of Health and by National Science Foundation grant PCM78-16298.

#### LITERATURE CITED

1. Becker, Y., H. Dym, and I. Sarov. 1968. Herpes simplex virus DNA. *Virology* **36**:184-192.
2. Clements, J. B., R. Cortini, and N. M. Wilkie. 1976. Analysis of herpesvirus DNA substructure by means of restriction endonucleases. *J. Gen. Virol.* **30**:243-256.
3. Delius, H., and J. B. Clements. 1976. A partial denaturation map of herpes simplex virus type 1 DNA: evidence for inversions of the unique DNA regions. *J. Gen. Virol.* **33**:125-133.
4. Grafstrom, R. H., J. C. Alwine, W. L. Steinhart, C. W. Hill, and R. W. Hyman. 1975. The terminal repetition of herpes simplex virus DNA. *Virology* **67**:144-157.
5. Hayward, G. S., R. J. Jacob, S. C. Wadsworth, and B. Roizman. 1975. Anatomy of herpes simplex virus DNA: evidence for four populations of molecules that differ in the relative orientation of their long and short components. *Proc. Natl. Acad. Sci. U.S.A.* **72**:4243-4247.
6. Helling, R. B., H. M. Goodman, and H. W. Boyer. 1974. Analysis of endonuclease R. *EcoRI* fragments of DNA from lambdoid bacteriophages and other viruses by agarose gel electrophoresis. *J. Virol.* **14**:1235-1244.
7. Hyman, R. W., S. Burke, and L. Kudler. 1967. A nearby inverted repeat of the terminal sequence of herpes simplex virus DNA. *Biochem. Biophys. Res. Commun.* **68**:609-615.
8. Jacob, R. J., L. S. Morse, and B. Roizman. 1979. Anatomy of herpes simplex virus DNA. XII. Accumulation of head-to-tail concatemers in nuclei of infected cells and their role in the generation of the four isomeric arrangements of viral DNA. *J. Virol.* **29**:448-457.
9. Kieff, E. D., S. L. Bachenheimer, and B. Roizman. 1971. Size, composition, and structure of the deoxyribonucleic acid of herpes simplex virus subtypes 1 and 2. *J. Virol.* **8**:125-132.
10. Knipe, D. M., W. T. Ruyechan, B. Roizman, and R. W. Honess. 1979. Molecular genetics of herpes simplex virus. IV. The terminal  $\alpha$  sequence of the L and S components are obligatorily identical and constitute a part of a structural gene mapping predominantly in the S component. *Proc. Natl. Acad. Sci. U.S.A.*, in press.
11. Little, J. W. 1967. An exonuclease induced by bacteriophage  $\lambda$ . *J. Biol. Chem.* **242**:679-686.
12. Locker, H., and N. Frenkel. 1979. Structure and origin of defective genomes contained in serially passaged herpes simplex virus type 1 (Justin). *J. Virol.* **29**:1065-1077.
13. Morse, L. S., T. G. Buchman, B. Roizman, and P. A. Schaffer. 1977. Anatomy of herpes simplex virus DNA. IX. Apparent exclusion of some parental DNA arrangements in the generation of intertypic (HSV-1  $\times$  HSV-2) recombinants. *J. Virol.* **24**:231-248.
14. Preston, V. G., A. J. Davison, H. S. Marsden, M. S. Timbury, J. H. Subak-Sharpe, and J. M. Wilkie. 1978. Recombinants between herpes simplex virus type 1 and 2: analysis of genome structures and expression of immediate early polypeptides. *J. Virol.* **28**:499-517.
15. Sheldrick, P., and N. Berthelot. 1974. Inverted repetitions in the chromosome of herpes simplex virus. *Cold Spring Harbor Symp. Quant. Biol.* **39**:667-678.
16. Skare, J., and W. C. Summers. 1977. Structure and function of herpesvirus genomes. II. *EcoRI*, *XbaI* and *HindIII* exonuclease cleavage sites on herpes simplex virus type 1 DNA. *Virology* **76**:581-596.
17. Southern, E. M. 1975. Detection of specific sequences among DNA fragments separated by gel electrophoresis. *J. Mol. Biol.* **98**:503-517.
18. Summers, W. C., and J. Skare. 1977. Nucleotide sequence arrangements in the genome of herpes simplex virus and their relation to insertion elements, p. 471-476. *In* A. I. Bukhari, J. A. Shapiro, and S. Adhya (ed.), DNA insertion elements, plasmids and episomes. Cold Spring Harbor Laboratory, Cold Spring Harbor, N.Y.
19. Wadsworth, S., G. S. Hayward, and B. Roizman. 1976. Anatomy of herpes simplex virus DNA. V. Terminally repetitive sequences. *J. Virol.* **17**:503-512.
20. Wadsworth, S., R. J. Jacob, and B. Roizman. 1975. Anatomy of herpes simplex virus DNA. II. Size, composition, and arrangement of inverted terminal repetitions. *J. Virol.* **15**:1487-1497.
21. Wagner, M. J., and W. C. Summers. 1978. Structure of the joint region and the termini of the DNA of herpes simplex virus type 1. *J. Virol.* **27**:374-387.
22. Wilkie, N. M. 1976. Physical maps for herpes simplex virus type 1 DNA for restriction endonucleases *Hind III*, *Hpa-I*, and *X. bad*. *J. Virol.* **20**:222-233.
23. Wilkie, N. M., and R. Cortini. 1976. Sequence arrangement in herpes simplex virus type 1 DNA: identification of terminal fragments in restriction endonuclease digests and evidence for inversions in redundant and unique sequences. *J. Virol.* **20**:211-221.